Radiation Protection Dosimetry (2020), pp. 1–10 doi:10.1093/rpd/ncaa112

# ASSESSING RADIATION EXPOSURE INSIDE THE EARTH'S ATMOSPHERE

Anastasia Tezari[1,2], Pavlos Paschalis[2], Helen Mavromichalaki[2,*], Pantelis Karaiskos[1], Norma Crosby[3] and Mark Dierckxsens[3]
[1]Medical Physics Laboratory, Faculty of Medicine, National and Kapodistrian University of Athens, 75 Mikras Asias Street, Goudi, 11527 Athens, Greece
[2]Athens Cosmic Ray Group, Faculty of Physics, National and Kapodistrian University of Athens, Panepistimioupolis, Zografos, 15784 Athens, Greece
[3] Royal Belgian Institute for Space Aeronomy, Ringlaan-3-Avenue Circulaire, 1180 Brussels, Belgium

*Corresponding author: emavromi@phys.uoa.gr

*Received 17 April 2020; revised 25 June 2020; editorial decision 19 July 2020; accepted 19 July 2020*

**The study of the particle showers created inside the Earth's atmosphere due to interactions of cosmic rays of solar and galactic origin is of great importance for the determination of the radiation impact on technological and biological systems. DYASTIMA is a Geant4-based software application that simulates the evolution of secondary particle cascades inside the atmosphere of Earth. DYASTIMA-R is a new feature especially created for assessing the exposure of flight-personnel and frequent flyers to cosmic radiation by performing calculations of radiobiological quantities, such as dose and equivalent dose rates for several air-flight scenarios. In this work, the validation of DYASTIMA/DYASTIMA-R, according to internationally accepted ICRP and ICRU standards, is discussed. Initial results for radiobiological quantities for several air-flight scenarios are also included. The results for specific scenarios calculated by DYASTIMA/DYASTIMA-R are provided as a federated product through the European Space Agency Space Situational Awareness Space Weather Service Centre Network.**

## INTRODUCTION

As primary cosmic rays propagate through the interplanetary medium, at some point they reach the Earth's magnetic field. Some of these particles penetrate the geomagnetic field and finally arrive at the top of our atmosphere, where they interact with the atmospheric molecules, nuclei and ions[1,2]. Several physical interactions take place, such as decay, elastic and inelastic scattering, ionisation, photoelectric effect, compton scattering, annihilation, pair production and bremsstrahlung radiation, resulting in the creation of secondary particles. These secondary particles, which are basically protons, neutrons, charged pions and kaons but also electrons, positrons, muons, neutrinos and photons, continue to interact either with each other or with the atmospheric molecules, creating the evolution of the so-called atmospheric showers[2–4].

The study of these cascades is essential for a better understanding of space weather phenomena and effects and can provide useful insights for the assessment of radiation effects on both technological and biological systems[5,6]. Typical examples can be radiation protection aviation of crews and passengers[7–10], as well as prevention of damage on avionics[11,12]. Air showers can also provide significant information about the primary cosmic ray particles and the cosmogenic nuclides production[13,14].

Atmospheric showers can be detected by balloons flying at different altitudes inside Earth's atmosphere or by a variety of ground-based detectors located at various geographic coordinates at several altitudes (ranging from sea level to mountain tops)[15], such as the global network of neutron monitors[16] or muon counters[17]. Nevertheless, the simulation of the atmospheric cascade is a critical tool, as most of the particle detectors, such as neutron and muon monitors, are ground-based and are usually sensitive to a specific type of particle. Furthermore, there are not enough adequate experimental data for all space weather conditions and phenomena[18,19]. As a result, the information collected from the detectors and the balloons at different atmospheric altitudes is not sufficient for the study of particle propagation through the atmosphere and its effects. Another great advantage of the simulations is to facilitate a realistic connection between the particle flux in the atmosphere with the actual particles that enter the atmosphere, providing all the necessary information in order to study all the physical processes of the cascade. Therefore, simulations allow the study of the shower evolution, the ionisation of the atmosphere, the interaction of the shower with a matter of the atmosphere as well as the calculation of several radiobiological quantities. Various programmes have been developed for this reason, with most of them making use of the well-known GEometry ANd Tracking (Geant4[20–22], or

FLUktuierende KAskade (FLUKA)[23,24] simulation toolkits.

A typical example is PLANETOCOSMICS, a Monte Carlo simulation in Geant4 of the evolution of the air showers inside the atmosphere[25,26]. Other models include the Cosmic Ray Ionisation Model for Ionosphere and Atmosphere (CORIMIA) and the Cosmic Ray Simulations for Kascade (CORSIKA), both developed in FLUKA. CORIMIA takes into account the ionization losses in the atmosphere and can be used for the study of cosmic-ray ionisation at atmospheric altitudes above 30 km for a specific time and location[27], while CORSIKA studies the low–energy cascade development below 30 km[28,29].

Moreover, various software applications and models have been developed for radiation dosimetry calculations, in order to assess the radiation effects induced by galactic and solar cosmic rays to space crews and aircrews[30]. Some typical examples are the Aviation Dosimetry (AVIDOS), the Nowcast of Atmospheric Ionizing Radiation System (NAIRAS), SIEVERT, CARI, the Space Environment Information System (SPENVIS) and the CALculated and Verified Aviation (CALVADOS). AVIDOS is a software application for the estimation of radiation exposure during a flight and is accessible through ESA's Space Weather portal[31]. SPENVIS is a useful web interface collecting various models of the space environment, developed by the Royal Belgian Institute for Space Aeronomy (BIRA-IASB), and is also available through ESA's portal[32]. NAIRAS is also a model for the prediction of radiation due to galactic cosmic rays and solar energetic particles, developed by the NASA Langley Research Centre[33]. CARI[34,35] and SIEVERT[36,37] are also easily operated computer programmes that perform calculations of the effective dose due to galactic cosmic radiation on an aircraft, developed at the Federal Aviation Administration Civil Aerospace Medical Institute and the Institute of Radioprotection and Nuclear Safety (IRSN), respectively. CALVADOS is a system for the determination of aircrew dose exposure by the German Aerospace Centre (DLR) already applied to the flight crew of the flying company LUFTHANSA[38].

Dynamic Atmospheric Shower Tracking Interactive Model Application (DYASTIMA) is also a software application for the study of secondary particle cascades inside the atmosphere, based on Geant4[4]. It is implemented by the Athens Cosmic Ray Group and is provided by the Athens Neutron Monitor Station (A.Ne.Mo.S.) portal (http://cosray.phys.uoa.gr/index.php/dyastima). The latest version includes DYASTIMA-R, a feature especially created for radiation dosimetry calculations inside the atmosphere of a planet[39–42]. The results for specific scenarios calculated by DYASTIMA and DYASTIMA-R are provided as a federated product through the European Space Agency Space Situational Awareness Space Weather Service Centre Network (http://swe.ssa.esa.int/web/guest/dyastima-federated).

In this work, the new version of DYASTIMA with the addition of DYASTIMA-R is used. Its validation process according to globally accepted standards is described. The initial results obtained by DYASTIMA and DYASTIMA-R are presented and discussed. Conclusions of the paper are summarised and potential next steps are given.

## DYASTIMA SOFTWARE

As mentioned above, DYASTIMA is a standalone application in Geant4 providing Monte Carlo simulations of the secondary cosmic ray particle cascades and the propagation of these particles through the atmosphere of Earth or generally through the atmospheric layers of a planet having its own atmosphere[4]. DYASTIMA, so far, has been successfully used for the study of the cascades in the atmosphere of Earth[4], the estimation of the ionisation of the Earth's atmosphere due to cosmic radiation during the ground level enhancement (GLE) on 17 May 2012 (GLE71)[43] as well as the calculation of the ion production rate in the atmosphere of Venus[44].

### DYASTIMA input and output parameters

DYASTIMA software is based on a user-friendly graphical user interface (GUI), which allows easy parameterization for a more accurate study of the cascade developing not only in Earth's atmosphere but also in the atmosphere of other planets[4,45]. The model requires several input parameters, all defined by the user. These parameters concern the general characteristics of the planet and its surrounding atmosphere, where the air showers are developed, such as its radius, its surface type and pressure, the components of the magnetic field (north, east and vertical) and the gravitational acceleration as well as the atmospheric structure and temperature profile. The primary cosmic ray spectra, i.e. the particle's type, the flux etc., is one of the most important input parameters of the simulation. The spectrum can be extracted by various models and tools such as the ISO model[46], CREME96[47–49] and Nymmik *et al*. model[50]. The Geant4 settings alongside with the simulation geometry settings should also be taken into consideration. These may include the geometry model of the simulation, the division of the atmosphere, the appropriate Geant4 physics list that best describes the physical interactions taking place between the primary and secondary cosmic ray particles and the atmospheric matter, as well as

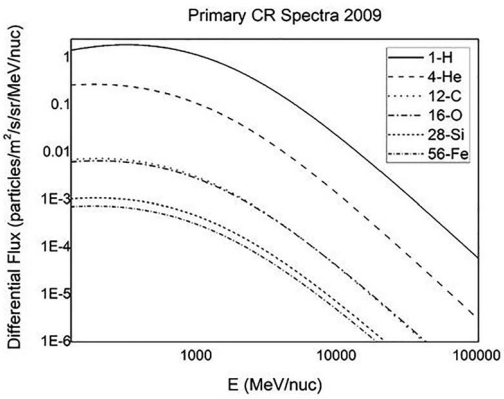


Figure 1: A typical example of the primary cosmic ray spectra for 6 elements ($^{1}$H, $^{4}$He, $^{12}$C, $^{16}$O, $^{28}$Si and $^{56}$Fe) used as an input parameter in DYASTIMA. This one is extracted by using the software tools OMERE and CRÈME for 2009 for a cut-off rigidity of 0 GV

the definition of the atmospheric altitudes where the tracking of particles will take place[4,39–42].

This large amount of information is processed during each simulation scenario, providing, as output, accurate values for various aspects of the developing cascade. These may be the number of the secondary particles present at different atmospheric altitudes, their energy and the energy deposition, as well as their direction and arrival time. All this information is separately collected for each particle type at each defined tracking layer.

In this work, the primary cosmic ray spectra for six chemical elements ($^{1}$H, $^{4}$He, $^{12}$C, $^{16}$O, $^{28}$Si and $^{56}$Fe) is based on the ISO15390[46] model for lower energies (below 10 MeV/nuc), and on Nymmik *et al*. model[50] for higher energies, as these models are quite similar for energies above 10 MeV/nuc. A typical spectrum used as input in DYASTIMA is shown in Figure 1. It should be noted that the primary spectra have been derived by using the OMERE software offered by TRAD[51]. The atmospheric profile, i.e. the temperature as a function of the atmospheric altitude, is based on the International Standard Atmosphere (ISA) model[52,53]. The mean annual values for the North, East and Vertical components of the magnetic field used in the simulation are provided by the National Oceanic and Atmospheric Administration, based on the IGRF model (https://www.ngdc.noaa.gov/geomag/) at mean sea level.

## DYASTIMA-R radiation dosimetry calculations

The radiation environment of the Earth's atmosphere, directly affected by space radiation, plays a key role in the safety of aircrews and passengers during commercial flights. The calculation of several radiometric quantities, such as the absorbed dose and the equivalent dose, is essential for the determination of human exposure to ionizing solar and galactic cosmic radiation during a flight.

For this reason, the DYASTIMA software is enhanced with DYASTIMA-R, a new feature performing radiation dosimetry calculations inside the atmosphere of Earth[39–42]. More specifically, DYASTIMA-R is a Monte Carlo simulation performed on a human phantom for the calculation of the dose and equivalent dose rates at different atmospheric altitudes during various flight scenarios covering various geographic coordinates and phases of solar activity. It should be noted that DYASTIMA-R is not an autonomous software, as it requires the output provided by DYASTIMA. The user can define the characteristics of the cylindrical phantom that simulates the human body, such as the dimension and the material, the number of iterations, i.e. the interactions of the collected particles with the phantom matter at each atmospheric altitude, and the reference Geant4 physics list. The radiation weighting factors used for the calculation of the equivalent dose rate are according to well-accepted international standards, as found in the International Commission on Radiological Protection (ICRP) Reports 103, 123 and 132[54,55].

## Validation of DYASTIMA-R

The quantities most widely used for the determination of the exposure limits to radiation are (1) the mean absorbed dose D (measured in Gray), corresponding to the mean energy deposited on a mass due to an ionizing radiation type, (2) the equivalent dose H (in Sievert), that takes into account each radiation type's radiobiological effectiveness, as well as (3) the effective dose E (also in Sievert), which considers additionally the type of tissue or organ being irradiated[54–56]. However, these quantities are not suitable for the radiation risk assessment during an air flight or a manned space mission, since they are not measurable quantities. For this reason, the ICRP and the International Commission on Radiation Units and Measurements (ICRU) recommend the use of other operational quantities, such as the ambient dose equivalent H*(10), also expressed in Sievert[54–57]. This is the equivalent dose at a point in a radiation field that would be produced by the corresponding expanded and aligned field in the ICRU sphere (a reference phantom of tissue-equivalent material[58]), at a depth of 10 mm on the radius vector opposing the direction of the aligned field.

Both ICRP 123 and ICRU Report 84 documents provide ambient dose equivalent reference data for

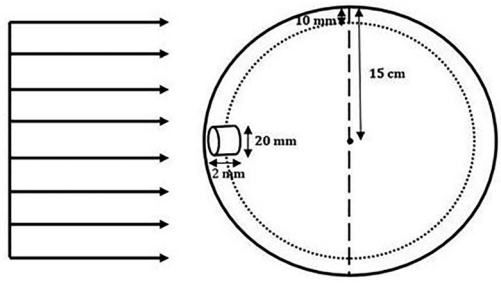


Figure 2: A schematic description of the dosimetry setup used for the validation of DYASTIMA-R

cosmic radiation exposure, which are actual measurements realised onboard flights from 1992 to 2006, and may be used for the assessment and validation of models and tools providing a calculation of radiation quantities for air flights[55,57]. The acceptable discrepancy limit recommended between the reference data and the model-calculated values are of the order of 30%. The flight scenarios based on these measurements and proposed by ICRP and ICRU cover three different time periods corresponding to different solar activity conditions (January 1998, January 2000, January 2002), 18 values of vertical geomagnetic cut-off rigidity with an increment of 1 GV (0–17 GV), and three flying altitudes, 9448.8 m/31 000 ft (FL310), 10 668.0 m/135 000 ft (FL350) and 11 887.2 m/39 000 ft (FL390), corresponding to the most frequent range of commercial aircraft flights. Many accredited tools and software applications, such as AVIDOS[31] and NAIRAS[33], have followed the above validation process. The validation of DYASTIMA and DYASTIMA-R, as required by ESA, has been presented successfully[59–61].

## DYASTIMA-R configuration

For the validation of DYASTIMA and DYASTIMA-R[59–61], a special version of DYASTIMA-R was implemented in order to calculate the operational quantity ambient dose equivalent H*(10). The dosimetry setup is according to the one already successfully used by Pelliccioni[62]. The ICRU sphere is used, instead of a human phantom, and a cylindrical volume of 10 mm radius and 2 mm width is placed at a depth of 10 mm from the sphere surface. The sphere is then illuminated, with the secondary particles collected at each atmospheric layer. A visual representation of this setup is given in Figure 2.

The atmospheric profile of Earth as well as the spectrum of the primary cosmic ray particles at the top of the Earth's atmosphere (86 km altitude) are two basic factors not only for the validation of DYASTIMA/DYASTIMA-R but also for their operation in general. More specifically, the ISA[52,53] and the ISO Galactic Cosmic Ray model[46] have been used for the description of Earth's atmosphere and the primary cosmic ray spectra, respectively.

The effect of the geomagnetic field for various geographic coordinates is introduced by the usage of the vertical cut-off rigidity values in the primary spectra calculations. These values represent the geomagnetic field's continuous evolution and are calculated with the International Geomagnetic Reference Field (IGRF) for Epoch 2000.0[63].

## Comparison with the reference data

DYASTIMA and DYASTIMA-R runs have been performed for all the flight scenarios proposed by ICRU (three time periods, 18 vertical cut-off rigidity values, three flying altitudes)[59–61]. The ambient dose equivalent values H*(10) obtained by simulations with DYASTIMA-R, as well as the ICRU reference data, as a function of the vertical geomagnetic cut-off rigidity threshold $R_c$ and the discrepancy for each time period (January 1998, January 2000, January 2002) are given in Tables 1–3. It is reminded that the acceptable percentage difference is 30%.

It is interesting to note that DYASTIMA-R values for cut-off rigidity thresholds ranging between 0 and 10 GV are in good agreement with the ICRU reference data, with a discrepancy generally not more than 30%. This range of cut-off rigidities corresponds to polar and middle geographic latitudes, covering almost 75% of the globe's surface. In equatorial regions, i.e. above 10 GV, a greater discrepancy of the order of up to 40% is observed, which is probably due to the more complicated geomagnetic field at this region. In these regions, DYASTIMA-R underestimates the H*(10) in agreement with other models[33,34]. A similar behaviour can also be observed in other models, with the H*(10) and the reference data being compatible up to 10 GV[33,34].

More specifically, during January 1998, corresponding to solar minimum conditions, the DYASTIMA-R obtained values and the reference data are almost identical for higher geographic latitudes (0–3 GV). The discrepancy increases for higher $R_c$ values (10–17 GV), varying from 30 to 40% and is greater in the case of the highest-flying altitude FL390. Moreover, in January 2000, which corresponds to the ascending phase of Solar Cycle 23, the discrepancy follows the same pattern as mentioned above. Finally, during January 2002, near solar maximum conditions, the DYASTIMA-R values are in very good accordance with the reference data up to 12 GV, with the discrepancy between the values being significantly lower compared to 1998 and 2000[56].

The observed differences may be attributed to the input parameters used in the DYASTIMA

**Table 1. DYASTIMA-R ambient dose equivalent H*(10) (microSv) as a function of geomagnetic vertical cut-off rigidity (Rc) for January 1998 (solar minimum) for three flight levels (FLs). The Diff (%) corresponds to the percentage difference between the values obtained from DYASTIMA-R and the reference data provided by ICRU Rep. 84.**

| | FL310 | | FL350 | | FL390 | |
|---|---|---|---|---|---|---|
| Rc (GV) | H*(10) (microSv) | Diff (%) | H*(10) (microSv) | Diff (%) | H*(10) (microSv) | Diff (%) |
| 0 | 4 | −6.5 | 5.3 | −10.2 | 6.8 | −10.8 |
| 1 | 3.9 | −8.8 | 5.1 | −11.4 | 6.9 | −6.7 |
| 2 | 3.9 | −2.8 | 4.8 | −11.9 | 6.3 | −10.5 |
| 3 | 3.2 | −15.4 | 4.3 | −16.7 | 5.4 | −17.9 |
| 4 | 2.9 | −17.7 | 3.8 | −20.2 | 4.7 | −21.7 |
| 5 | 2.5 | −22.3 | 3.3 | −25 | 4 | −28.1 |
| 6 | 2.2 | −22.6 | 2.9 | −28.4 | 3.6 | −29 |
| 7 | 2 | −26.5 | 2.5 | −31.5 | 3.1 | −32.2 |
| 8 | 1.7 | −31.7 | 2.2 | −32 | 2.6 | −35.7 |
| 9 | 1.6 | −29.5 | 1.9 | −35.3 | 2.4 | −36.4 |
| 10 | 1.5 | −29.3 | 1.9 | −31 | 2.2 | −34.5 |
| 11 | 1.3 | −33.7 | 1.7 | −33.5 | 2 | −34.2 |
| 12 | 1.2 | −32.7 | 1.6 | −30.4 | 1.9 | −33.2 |
| 13 | 1.1 | −35.8 | 1.4 | −31.6 | 1.7 | −35.2 |
| 14 | 1.1 | −33 | 1.3 | −37 | 1.5 | −38.8 |
| 15 | 1 | −35.3 | 1.2 | −36.3 | 1.4 | −40.7 |
| 16 | 0.9 | −39.1 | 1.2 | −36.9 | 1.3 | −39.9 |
| 17 | 0.9 | −41.2 | 1.1 | −37.5 | 1.3 | −41.4 |

**Table 2. DYASTIMA-R ambient dose equivalent H*(10) (microSv) as a function of geomagnetic vertical cut-off rigidity (Rc) for January 2000 (solar transition) for three FLs. The Diff (%) corresponds to the percentage difference between the values obtained from DYASTIMA-R and the reference data provided by ICRU Rep. 84.**

| | FL310 | | FL350 | | FL390 | |
|---|---|---|---|---|---|---|
| Rc (GV) | H*(10) (microSv) | Diff (%) | H*(10) (microSv) | Diff (%) | H*(10) (microSv) | Diff (%) |
| 0 | 3.3 | −17.4 | 4.4 | −15.6 | 5.7 | −10.9 |
| 1 | 3.3 | −15.7 | 4.5 | −12.5 | 5.5 | −12.6 |
| 2 | 3.1 | −16.6 | 4.3 | −11 | 5.2 | −13.4 |
| 3 | 2.9 | −16.6 | 3.7 | −18.5 | 4.6 | −18.4 |
| 4 | 2.5 | −22.8 | 3.5 | −16.7 | 4.1 | −22.1 |
| 5 | 2.4 | −20.7 | 3.1 | −21.1 | 3.7 | −22.9 |
| 6 | 2.1 | −25.7 | 2.7 | −26.1 | 3.2 | −27.1 |
| 7 | 1.8 | −27.8 | 2.3 | −30.1 | 2.8 | −30.1 |
| 8 | 1.6 | −29.1 | 2.1 | −29.2 | 2.6 | −27.3 |
| 9 | 1.5 | −30.6 | 2 | −27.4 | 2.3 | −31.7 |
| 10 | 1.4 | −31.7 | 1.7 | −31 | 2.1 | −29.9 |
| 11 | 1.2 | −35.7 | 1.6 | −29.8 | 1.9 | −32.4 |
| 12 | 1.1 | −33.5 | 1.5 | −34.1 | 1.7 | −34.4 |
| 13 | 1 | −38.5 | 1.3 | −37.6 | 1.6 | −36.4 |
| 14 | 1 | −40.4 | 1.2 | −38.2 | 1.5 | −37.8 |
| 15 | 0.9 | −40.3 | 1.1 | −39.6 | 1.4 | −40.5 |
| 16 | 0.9 | −42.6 | 1 | −41.8 | 1.3 | −42.1 |
| 17 | 0.8 | −43.8 | 1 | −42 | 1.2 | −43.2 |

simulation. For example, the ISA is not suitable for use in the polar and equatorial regions, since it is based on average conditions for middle geographic latitudes[52,53]. Other models describing the characteristics of the atmosphere are also semi-empirical. Additionally, since the primary cosmic ray spectra can be derived through various models and software tools, substantial differences may

**Table 3. DYASTIMA-R ambient dose equivalent H*(10) (microSv) as a function of geomagnetic vertical cut-off rigidity (Rc) for January 2002 (solar maximum) for three FLs. The Diff (%) corresponds to the percentage difference between the values obtained from DYASTIMA-R and the reference data provided by ICRU Rep. 84.**

| | FL310 | | FL350 | | FL390 | |
|---|---|---|---|---|---|---|
| Rc (GV) | H*(10) (microSv) | Diff (%) | H*(10) (microSv) | Diff (%) | H*(10) (microSv) | Diff (%) |
| 0 | 3.3 | −10.2 | 4.5 | −4.1 | 5.2 | −8.5 |
| 1 | 3.2 | −11.5 | 4.3 | −6.9 | 5.3 | −5.5 |
| 2 | 3 | −11.1 | 3.9 | −10.2 | 5.1 | −3.8 |
| 3 | 2.8 | −14.6 | 3.9 | −5.5 | 4.7 | −6.6 |
| 4 | 2.4 | −20.5 | 3.3 | −15.1 | 3.9 | −16.1 |
| 5 | 2.3 | −18.6 | 2.9 | −19.5 | 3.7 | −14.7 |
| 6 | 2 | −25 | 2.6 | −19.8 | 3.1 | −22 |
| 7 | 1.8 | −25.1 | 2.3 | −24.7 | 2.7 | −27.6 |
| 8 | 1.6 | −25.6 | 2.1 | −23.8 | 2.5 | −26.4 |
| 9 | 1.5 | −30.8 | 1.9 | −26.4 | 2.2 | −29.5 |
| 10 | 1.3 | −31.9 | 1.7 | −28.1 | 2 | −30.4 |
| 11 | 1.2 | −32.7 | 1.6 | −27.1 | 1.9 | −30.4 |
| 12 | 1.2 | −29.9 | 1.5 | −30.5 | 1.7 | −33 |
| 13 | 1 | −36.7 | 1.4 | −31.8 | 1.6 | −34.1 |
| 14 | 1 | −37 | 1.2 | −37.4 | 1.5 | −32.9 |
| 15 | 0.9 | −38.7 | 1.2 | −37.7 | 1.4 | −38.2 |
| 16 | 0.9 | −42.1 | 1.1 | −37.7 | 1.3 | −42.2 |
| 17 | 0.8 | −42.5 | 1 | −43.2 | 1.2 | −43.5 |

present not only in the lower energies but also in computational aspects, such as the definition of a single $R_c$ orbit. For these reasons, DYASTIMA is under constant improvement and in the pursuit of more appropriate input parameters in order to provide more precise results.

## INITIAL RESULTS

The ionizing energy deposition on the different atmospheric layers due to the evolving cascade of secondary particles is calculated for solar minimum conditions (2008) as well as during solar maximum conditions (2014), and the results are presented in Figure 3. It is observed that the evolution of the cascade starts at ∼40 km altitude inside the atmosphere and reaches its peak at 13 and 12 km altitude for 2008 and 2014, respectively, where the maximum energy deposition takes place. The average altitude corresponding to the majority of commercial air-flights is at 10–12 km, and therefore it is necessary to perform radiation dosimetry calculations at these altitudes.

The average ambient equivalent dose rate per year as a function of altitude is given in Figure 4, for 2 years (2008 and 2014) that correspond to different phases of solar activity. It is observed that H*(10) increases up to 40 km altitude (roughly the altitude where the cascade begins) and then it remains averagely constant. Furthermore, the dose rate is significantly higher during 2008 that

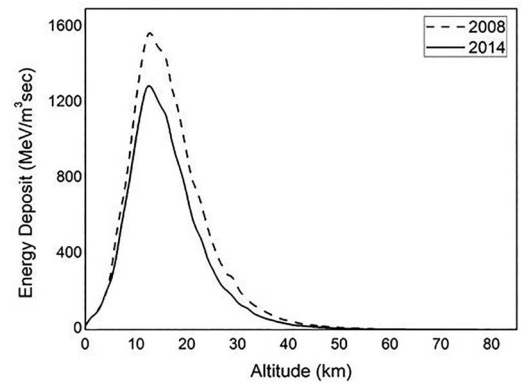


Figure 3: The ionizing energy deposition in the atmospheric matter for 2008 (solar minimum conditions) and 2014 (solar maximum conditions) as calculated by DYASTIMA software

corresponds to solar minimum conditions, due to the anticorrelation of the solar activity and the galactic cosmic ray intensity.

The average ambient dose equivalent H*(10) rate (in microSv per hour) on an annual basis, as calculated by DYASTIMA-R during Solar Cycle 24 for a rigidity threshold of 0 GV for the three most frequent flying altitudes (FL310, FL350, FL390), is presented in Figure 5. The higher dose rate is observed during 2009[64], the solar minimum between

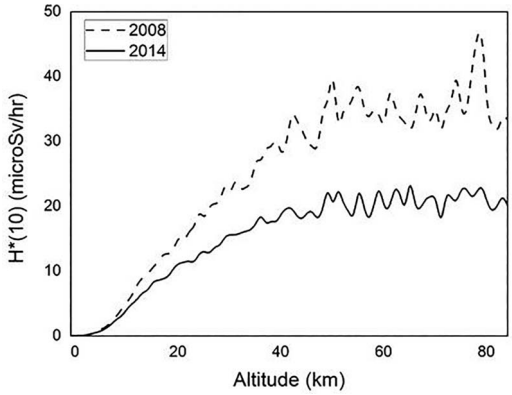


Figure 4: The ambient dose equivalent H*(10) rate as a function of altitude, covering the whole atmosphere of Earth, for 2008 and 2014, as calculated by DYASTIMA-R

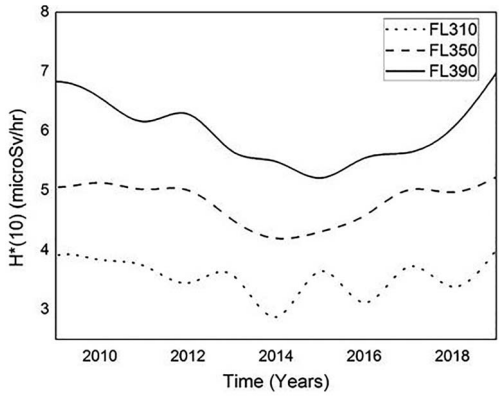


Figure 5: The ambient dose equivalent H*(10) rate during Solar Cycle 24 as calculated by DYASTIMA-R for a cut-off rigidity of 0 GV, for three different flying altitudes (FL310, FL350, FL390)

Solar Cycles 23 and 24, while the lower dose and ambient equivalent dose rate take place during the solar maximum of Solar Cycle 24 (2014), indicating once more the anticorrelation between cosmic ray intensity and solar activity. Generally, the dose rate presents very little variation in the equatorial regions during the solar cycle, but a higher variation at higher latitudes[34]. Hereby, it can be observed that this effect is more evident for higher altitudes (FL390) at polar regions (0 GV). The average ambient dose equivalent H*(10) rate as a function of the cut-off rigidity threshold Rc for 2002, for three flying altitudes, is presented in Figure 6. The dose rate dependence of the geographic latitude is evident, as H*(10) decreases with the increasing of the rigidity threshold[65].

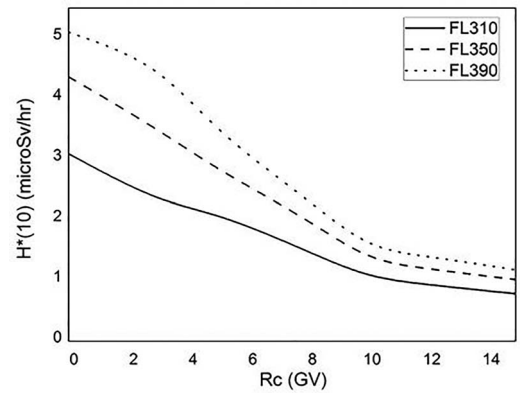


Figure 6: The ambient dose equivalent H*(10) rate as a function of the cut-off rigidity threshold Rc for 2002 as calculated by DYASTIMA-R, for three different flying altitudes (FL310, FL350, FL390)

## CONCLUSIONS AND NEXT STEPS

Currently, there is constant growth in the number of air flights since more and more passengers choose flying as a mean of transportation, increasing eventually air traffic. For this reason, many aircrafts are obliged to fly at higher atmospheric altitudes or even altering their routes, resulting in a higher radiation accumulation due to cosmic rays for both the aircraft crew and the passengers[65]. Additionally, there is also an increase in trans-polar flights, where the radiation exposure is significantly higher. Therefore, the calculation of quantities useful for radiation assessment is very important, especially for higher geographic latitudes, as more particles can penetrate through the atmosphere due to the lower cut-off rigidity threshold.

DYASTIMA-R is validated according to the standards provided by ICRP 123 and ICRU Report 84 documents. Dosimetry calculations were performed for three flying altitudes, 18 vertical cut-off rigidities and three-time stamps, which correspond to different periods of solar activity (solar maximum, ascending phase and solar maximum of Solar Cycle 23). From the above analysis, it is concluded that DYASTIMA/DYASTIMA-R meet on a satisfactory level the criteria proposed by ICRP and ICRU as the discrepancy observed between the reference data and the calculated values does not exceed in general the acceptable limit of 30%. Therefore, DYASTIMA-R can be used for reliable dosimetry calculations of the exposure of aviators and passengers to ionizing cosmic radiation during air flights.

The preliminary results are also very promising for better understanding the evolution of the secondary particle cascade inside the atmosphere and the determination of the radiation exposure at different

atmospheric layers. DYASTIMA and DYASTIMA-R may be useful software tools for radiation dosimetry calculations inside the atmospheres of other planets as well. The GUI of DYASTIMA makes the software accessible and user-friendly allowing easy parameterization, so it can be used by entities concerned with the radiation effects on aircrews, frequent travellers, legislators, etc., either for scientific or educational purposes.

So far, DYASTIMA-R radiation dosimetry calculations are performed for specific points inside the atmosphere defined by atmospheric altitude, geographic coordinates and magnetic rigidity threshold dosimetry calculations. The following phase will include dosimetry calculations during a whole flight, by taking into account the flight route as well as the duration of the flight. The structure of the airplane as a parameter is also under further consideration. Therefore, DYASTIMA-R will soon be enhanced by more flight scenarios by performing a long-term analysis, covering a wider range of different solar activity periods, as well as different rigidity thresholds, covering most of the geographic coordinates. DYASTIMA/DYASTIMA-R will be also applied for radiation dosimetry calculations during different Space Weather events of high temporal variability, such as GLEs. During such events, the exposure at aircraft altitudes is significantly increased, since the cosmic ray intensity may increase several orders of magnitude in minutes[66–70].

DYASTIMA is based on a friendly GUI, offering free parameterization to the user. The user can define the characteristics of the planet and the simulation, the primary cosmic ray spectra and the atmospheric profile. The spectrum may be derived by various models and tools such as the ISO model[46], CREME96[47–49] and Nymmik *et al*. model[50]. The characteristics of the atmosphere can also be provided, by several models, such as the ISA, the Mass-Spectrometer-Incoherent-Scatter (NRLMSISE-00), Marshall Engineering Thermosphere (MET-V 2.0) or the Drag Temperature Model (DTMB78). Most of these models are semi-empirical. Therefore, differences may occur, depending on the model chosen by the user.

In summary, DYASTIMA provides all the important parameters for the description of the cascade, such as the type and the number of the secondary particles, their direction and arrival time, as well as the energy and the energy deposit at different atmospheric altitudes. Based on all these parameters, radiation dosimetry calculations can be performed. All this information can be either derived as a whole, or for each particle type of the cascade individually. This allows to study the atmospheric showers at other planets too. Next steps will also include the simulation of the atmospheric cascades in other planets, such as the atmosphere of Mars, as it may provide the necessary information needed to evaluate the radiation exposure of spacecraft crews due to cosmic radiation in future manned missions.

## ACKNOWLEDGEMENTS

This work is supported by ESA SSA SWE Space Radiation Expert Service Centre activities (ESA contract number 4000113187/15/D/MRP). The European Neutron Monitor Services research is funded by the ESA SSA SN IV-3 Tender: RFQ/3-13556/12/D/MRP. A.Ne.Mo.S is supported by the Special Research Account of Athens University (70/4/5803). A.T. thanks the Hellenic State Scholarship Foundation (IKY) for supporting her with a doctoral scholarship through the Operational Programme <<Human Resources Development, Education and Lifelong learning>> in the context of the project 'Strengthening Human Resources Research Potential via Doctorate Research – 2nd Cycle' (MIS-5000432), co-financed by Greece and the European Union (European Social Fund- ESF).

## CONFLICT OF INTEREST

The authors declare that there is no conflict of interest.

## REFERENCES

1. Dorman, L. I. Cosmic Rays in the Earth's Atmosphere and Underground. New York: Kluwer Academic Publishers (2004).
2. Singh, A. K., Singh, D. and Singh, R. P. *Impact of galactic cosmic rays on Earth's atmosphere and human health*. Atmos. Environ. **45**, 3806–3818 (2011).
3. Kudela, K. *On energetic particles in space*. Acta Phys. Slovaca **59**, 537–652 (2009).
4. Paschalis, P., Mavromichalaki, H., Dorman, L. I., Plainaki, C. and Tsirigkas, D. *Geant4 software application for the simulation of cosmic ray showers in the Earth's atmosphere*. New Astron. **33**, 26–37 (2014).
5. Lilensten, J. and Belehaki, A. *Developing the scientific basis for monitoring, modelling and predicting space weather*. Acta Geophys. **57**, 1–14 (2009).
6. Kudela, K., Storini, M., Hofer, M. Y. and Belov, A. *Cosmic rays in relation to space weather*. Space Sci. Rev. **93**, 153–174 (2000).
7. Cucinotta, F. A. and Durante, M. *Cancer risk from exposure to galactic cosmic rays: implications for space exploration by human beings*. Lancet Oncol. **7**, 431–435 (2006).
8. Beck, P., Barlett, D., Lindborg, L., McAulay, I., Schnuer, K., Schraube, H. and Spurny, F. *Aircraft crew radiation workplaces: comparison of measured and calculated ambient dose equivalent rate data using the EURADOS in-flight radiation data base*. Radiat. Prot. Dosimetry **118**(2), 182–189 (2006).

9. Beck, P., Latocha, M., Dorman, L., Pelliccioni, M. and Rollet, S. *Measurements and simulations of the radiation exposure to aircraft crew workplaces due to cosmic radiation in the atmosphere*. Radiat. Prot. Dosimetry **126**(1–4), 564–567 (2007).
10. European Radiation Dosimetry Group (EURADOS). Cosmic radiation exposure of aircraft crew - Compilation of measured and calculated data, EU Commission Radiation Protection Issue No. 140 Lindborg, L., Bartlett, D. T., Beck, P., McAulay, I. R., Schnuer, K., Schraube, K. and Spurný, F., Eds. (2004) (ISBN 92-894-8448-9).
11. Baker, D. N., Daly, E., Daglis, I., Kappenman, J. G. and Panasyuk, M. *Effects of space weather on technology infrastructure*. Space Weather **2**(2) (2004).
12. Bothmer, V. and Daglis, I. Space Weather. Physics and Effects (Springer Praxis). (Chichester, UK: Praxis Publishing Ltd) (2007).
13. Kovaltsov, G. A., Mishev, A. and Usoskin, I. G. *A new model of cosmogenic production of radiocarbon $^{14}C$ in the atmosphere*. EarthPlanet. Sc. Lett. **114**(337), 120–338 (2012).
14. Poluianov, S. V., Kovaltsov, G. A., Mishev, A. and Usoskin, I. G. *Production of cosmogenic isotopes $^{7}Be$, $^{10}Be$, $^{14}C$, $^{22}Na$, and $^{36}Cl$ in the atmosphere: altitudinal profiles of yield functions*. J. Geophys. Res. Atmos. **121**, 8125–8136 (2016).
15. Bütikofer, R. Ground-Based Measurements of Energetic Particles by Neutron Monitors. In: Solar Particle Radiation Storms Forecasting and Analysis. Astrophysics and Space Science Library. Vol. **444**. Malandraki, O. and Crosby, N., Eds. (Cham: Springer) (2018).
16. Mavromichalaki, H. *et al. Applications and usage of the real—time neutron monitor database*. Adv. Space Res. **47**, 2210–2222 (2011).
17. Supanitsky, A. D., Etchegoyen, A., Medina-Tanco, G., Allekotte, I., Gómez Berisso, M. and Medina, M. C. *Underground muon counters as a tool for composition analyses*. Astropart. Phys. **29**(6), 461–470 (2008).
18. Eroshenko, E., Velinov, P., Belov, A., Yanke, V., Pletnikov, E., Tassev, Y. and Mishev, A. Relationships between cosmic ray neutron flux and rain flows. In: Proc. 21th ECRS. (2008).
19. Mares, V., Brall, T., Bütikofer, R. and Rühm, W. *Influence of environmental parameters on secondary cosmic ray neutrons at high-altitude research stations at Jungfraujoch, Switzerland, and Zugspitze, Germany*. Radiati. Phys. Chem. **168**, 108557 (2020).
20. Agostinelli, S. *et al. Geant4—a simulation toolkit*. Nucl. Instrum. Methods A **506**, 250–303 (2003).
21. Allison, J., Amako, K., Apostolakis, J. *et al. Geant4 developments and applications*. IEEE Trans. Nuclear Sci **53**, 270–278 (2006).
22. Allison, J. *et al. Recent developments in Geant4*. Nucl. Instrum. Methods A **835**, 186–225 (2016).
23. Ferrari, A., Sala, P. R., Fasso, A. and Ranft, J. *A multi-particle, transport code,* CERN-2005-10, INFN/TC_05/11, SLAC-R-773 (2005).
24. Battistoni, G., Ferrari, A., Montaruli, T. and Sala, P. R. *The FLUKA atmospheric neutrino flux calculation*. Astropart. Phys. **19**, 269 (2003).
25. Desorgher, L. *et al. Atmocosmics: a GEANT4 code for computing the interaction of cosmic rays with the Earth's atmosphere*. Int. J. Mod. Phys. A **20**(29), 6802–6904 (2005).
26. Usoskin, I., Desorgher, L., Velinov, P. I. Y., Storini, M., Flueckiger, E., Buetikofer, R. and Kovaltsov, G. A. *Solar and galactic cosmic rays in the Earth's atmosphere*. Acta Geophys. **57**, 88–101 (2009).
27. Velinov, P. I. Y., Asenovski, A., Kudela, K., Lastovicka, J., Mateev, L., Mishev, A. and Tonev, P. *Impact of cosmic rays and solar energetic particles on the Earth's ionosphere and atmosphere*. J. Space Weather Space Clim. **3**, A14 (2013).
28. Heck, D., Knapp, J., Capdevielle, J. N., Schatz, G. and Thouw, T. CORSIKA: a Monte Carlo code simulate extensive air showers, Forschumgszentrum Karlsruhe GmbH, V +90P., TIB Hannover, D-30167 Hannover, Germany (1998).
29. Velinov, P. I. Y. and Mishev, A. *Cosmic ray induced ionization in the atmosphere estimated with CORSIKA code simulations*. C. R. Acad. Bulg. Sci. **60**(5), 493–500 (2007).
30. European Commission. *Comparison of codes assessing radiation exposure of aircraft crew due to galactic cosmic radiation*, Directorate-General for Energy, Directorate D—Nuclear Safety & Fuel Cycle, Unit D4—Radiation Protection. (2012).
31. Latocha, M., Beck, P. and Rollet, S. *AVIDOS—a software package for European accredited aviation dosimetry*. Radiat. Prot. Dosimetry **136**(4), 286–290 (2009).
32. SPENVIS, https://www.spenvis.oma.be/, (accessed 30 August 2019).
33. Mertens, C. J., Meier, M. M., Brown, S., Norman, R. B. and Xu, X. *NAIRAS aircraft radiation model development, dose climatology, and initial validation*. Space Weather **11**, 603–635 (2013).
34. Friedberg, W., Copeland, K., Duke, F. E., O'Brien, K. and Darden, E. B. Jr. *Guidelines and technical information provided by the US federal aviation administration to promote radiation safety for air carrier crew members*. Radiat. Prot. Dosimetry **86**, 323–327 (1999).
35. CARI, http://jag.cami.jccbi.gov/cariprofile.asp, (accessed 30 August 2019).
36. IRNS. *Scientific and technical report*. IRNS. **4**, 121–124 (2002).
37. SIEVERT, https://www.sievert-system.org/, (accessed 30 August 2019).
38. Berger, T., Meier, M., Reitz, G. and Schridde, M. *Long-term dose measurements applying a human anthropomorphic phantom onboard an aircraft*. Radiat. Meas. **43**, 580–584 (2008).
39. Paschalis, P., Tezari, A., Gerontidou, M. and Mavromichalaki, H. *A new tool for radiation exposure calculations in aircraft flights during disturbed solar activity periods*. EGU, Vienna, Austria, (2016).
40. Paschalis, P., Tezari, A., Gerontidou, M., Mavromichalaki, H. and Nikolopoulou, P. *Space radiation exposure calculations during different solar and galactic cosmic ray activities*, XXV European Cosmic Ray Symposium. (2016).
41. Paschalis, P., Tezari, A., Gerontidou, M., Mavromichalaki, H. and Ioannidou, S. Space radiation exposure simulation during different phases of solar activity. In: HPS 50th Midyear Meeting. (Bethesda, Maryland, USA) (2017).

42. Paschalis, P., Tezari, A., Gerontidou, M., Mavromichalaki, H. and Karaiskos, P. Radiation exposure of aircrews due to Space Radiation. In: Proc. 27th HNPS Annual Symposium. (Athens, Greece) (2018).
43. Dorman, L. I., Paschalis, P., Plainaki, C. and Mavromichalaki, H. Estimation of the cosmic ray ionization in the Earth's atmosphere during GLE71. Proc. 34th International Cosmic Ray Conference, Hague, The Netherlands, (2015).
44. Plainaki, C., Paschalis, P., Grassi, D., Mavromichalaki, H. and Andriopoulou, M. *Interactions of cosmic rays with the Venusian atmosphere during different solar activity conditions*. Ann. Geophys. **34**, 595–608 (2016).
45. Athens Cosmic Ray Group. *DYASTIMA Software User Manual*. (2019). Accessible at http://cosray.phys.uoa.gr/apps/DYASTIMA/DYASTIMA_USER_MANUAL.pdf.
46. International Organization for Standardization (ISO). *Space environment (natural and artificial)—Galactic cosmic ray model*. **15390**, 2004 (2004).
47. Tylka, A. J., Adams, J. H., Boberg, P. R. Jr., Brownstein, B., Dietrich, W. F., Flueckiger, E. O., Petersen, E. L., Shea, M. A., Smart, D. F. and Smith, E. C. *CREME96: a revision of the cosmic ray effects on micro-electronics code*. IEEE Trans. Nucl. Sci. **44**, 2150–2160 (1997).
48. Weller, R. A., Mendenhall, M. H., Reed, R. A., Schrimpf, R. D., Warren, K. M., Sierawski, B. D. and Massengill, L. W. *Monte Carlo simulation of single event effects*. IEEE Trans. Nucl. Sci. **57**, 1726–1746 (2010).
49. Mendenhall, M. H. and Weller, R. A. *A probability-conserving cross-section biasing mechanism for variance reduction in Monte Carlo particle transport calculations*. Nucl. Instrum. Methods A **667**, 38–43 (2012).
50. Nymmik, R. A., Panasyuk, M. I. and Suslov, A. A. *Galactic cosmic ray flux simulation and prediction*. Adv. Space Res. **17**(2), 19–30 (1996).
51. OMERE. http://www.trad.fr/en/space/omere-software/ (accessed 30 August 2019).
52. International Civil Aviation Organization (ICAO). Manual of The ICAO Standard Atmosphere. In: Doc 7488-CD third ed. (1993).
53. International Organization for Standardization (ISO). *Standard Atmosphere*. **2533**, 1975 (2007). https://www.iso.org/standard/7472.html.
54. International Commission on Radiological Protection (ICRP). The. *Recommendations of the International Commission on Radiological Protection*. Ann. ICRP 37 **103** (2007, 2007).
55. International Commission on Radiological Protection (ICRP). *Assessment of Radiation Exposure of Astronauts in Space*. Ann. ICRP **42**(4), 123 (2013).
56. International Commission on Radiological Protection (ICRP). *Radiological protection from cosmic radiation in aviation*. Ann. ICRP **45**(1), 132 (2016).
57. International Commission on Radiation Units and Measurements (ICRU). *Reference data for the validation of doses from cosmic-radiation exposure of aircraft crew*. J Int Comm Radiat Units Meas 10(2), Report 84, Oxford University Press (2010).
58. International Commission on Radiation Units and Measurements (ICRU). *Radiation quantities and units*. J Int Comm Radiat Units Meas **33** (1980). ICRU Report 33.
59. Tezari, A., Paschalis, P., Mavromichalaki, H., Karaiskos, P., Crosby, N. and Dierckxsens, M. *DYASTIMA: simulating air showers in the atmosphere of a planet*. Proc. 70th IAC, Washington, DC, (2019).
60. ESA. *ESA SSA P3 SWE-III Acceptance Test Report*, R.137 Dynamic Atmospheric Tracking Interactive Model Application (DYASTIMA). (2019).
61. Paschalis, P., Tezari, A., Mavromichalaki, H., Crosby, N. and Dierckxsens, M. *Validation of DYASTIMA and integration to ESA SSA R-ESC*. 16th ESWW, Liege, Belgium, (2019).
62. Pelliccioni, M. *Overview of Fluence-to-effective dose and Fluence-to-ambient dose equivalent conversion coefficients for high energy radiation calculated using the FLUKA code*. Radiat. Prot. Dosimetry **88**(4), 279–297 (2000).
63. Smart, D.F. and Shea, M.A. *World grid of calculated cosmic ray vertical cutoff rigidities for epoch 2000.0*. Proc. 30th ICRC, Mexico, 2007.
64. Mrigakshi, A. I., Matthiä, D., Berger, T., Reitz, G. and Wimmer-Schweingruber, R. F. *Estimation of galactic cosmic ray exposure inside and outside the Earth's magnetosphere during the recent solar minimum between solar cycles 23 and 24*. Adv. Space Res. **52**, 979–987 (2013).
65. Jones, J. B. L., Bentley, R. D., Hunter, R., Iles, R. H. A., Taylor, G. C. and Thomas, D. J. *The practical issues of utilizing a european space weather programme for airline operations*. Proc. ESA space weather workshop, 194 (2001).
66. Matthiä, D., Heber, B., Reitz, G., Sihver, L., Berger, T. and Meier, M. *The ground level event 70 on December 13th, 2006 and related effective doses at aviation altitudes*. Radiat. Prot. Dosimetry **136**(4), 304–310 (2009).
67. Copeland, K. and Atwell, W. *Flight safety implications of the extreme solar proton event of 23 February 1956*. Adv. Space Res. **63**, 665–671 (2019).
68. Mishev, A. and Usoskin, I. *Numerical model for computation of effective and ambient dose equivalent at flight altitudes-application for dose assessment during GLEs*. J Space Weather Space Climate **5**, A10 (2015).
69. Mishev, A., Adibpour, F., Usoskin, I. and Felsberger, E. *Computation of dose rate at flight altitudes during ground level enhancements no. 69, 70 and 71. Flight safety implications of the extreme solar proton event of 23 February 1956. Adv*. Space Res. **55**(1), 354–362 (2015).
70. Flückiger, E. and Bütikofer, R. *Radiation doses along selected flight profiles during two extreme solar cosmic ray events*. Astrophys. Space Sci. Trans. **7**(2), 105–109 (2011).